ICANS-VI
INTERNATIONAL COLLABORATION ON ADVANCED NEUTRON SOURCES
June 27 - July 2, 1982

HIGH-ENERGY FISSION MODELS VALIDATION AND COMPARISON WITH EXPERIMENTS

T.W. Armstrong*, P. Cloth, D. Filges, R.D. Neef

Institut für Reaktorentwicklung
Kernforschungsanlage Jülich GmbH
Postfach 1913
D-5170 Jülich 1, Germany

*KFA Consultant, P.O. Box 2807
La Jolla, California 92038, USA

ABSTRACT

Calculations including the high energy fission models were performed. Comparisons on BNL-Cosmotron arrangements of thermal neutron peak fluxes in the H_2O-moderator for lead and depleted uranium targets are given for different proton beam energies (540, 960, 1470 MeV) and two B_0-parameters (8 and 14 MeV) of the level density formula. Preliminary results of neutron spectra measurements for thin uranium targets are compared with HETC calculations at 590 MeV incident proton beam energy. The residual mass distributions are determined in thin uranium targets for proton beam energies of 0.3, 1.0, and 2.9 GeV. The calculations are done using the Rutherford and Appleton Laboratory high energy fission model (RAL) and are compared with respective calculations of the ORNL-model by Alsmiller et.al..

HIGH-ENERGY FISSION MODELS VALIDATION AND COMPARISON WITH EXPERIMENTS

T.W. Armstrong*, P. Cloth, D. Filges, R.D. Neef

Institut für Reaktorentwicklung
Kernforschungsanlage Jülich GmbH
Postfach 1913
D-5170 Jülich 1, Germany

*KFA Consultant, P.O. Box 2807
La Jolla, California 92038, USA

1. INTRODUCTION

From previous papers Ref. /1/ and /2/ at ICANS-V of the comparison of high energy fission (HEF) models for the High-Energy-Transport-Code (HETC) it was stated: Spectrum hardening with high energy fission models incorporated in the HET code is evident. The neutron captures in water surrounding finite depleted uranium targets are found to be 5-10 % higher with HEF. Significant differences of Rutherford and Appleton Laboratory (RAL) /3/ and the Oak Ridge National Laboratory (ORNL) /4/ high energy fission (HEF) models are found at incident proton beam energies above 1 GeV. The RAL model gives lower values than the ORNL model. The B_0 value seems to be model and energy dependend.

These investigations were continued studying the spatial dependence and thermal neutron peak fluxes in BNL-Cosmotron experiments (Refs. 5, 6). Preliminary comparisons for thin target measurements on uranium /Ref. 7/ with HETC calculations and predictions for residual mass distributions were also performed.

2. SPATIAL DEPENDENCE AND THERMAL NEUTRON PEAK FLUXES IN BNL-COSMOTRON EXPERIMENTS

The calculations were done for BNL-Cosmotron setups /5, 6/ at three proton beam energies (540, 960, and 1470 MeV) using HETC-, MORSE-CG-, and SIMPEL-spallation computer code system at KFA-IRE as described in Ref. 8. In Table 1 comparisons of the thermal peak fluxes in the H_2O-moderator for lead and uranium targets for different beam energies and several B_0-parameters of the level density formula are shown. In Table 2 the ratios of thermal peak fluxes for uranium and lead with different B_0-parameters are calculated.

In Fig. 1 the thermal peak fluxes for neutrons (n cm^{-2} s^{-1}) per proton are plotted as a function of proton beam energy for lead and uranium target with B_0=14. The uranium target system gives twice the thermal neutron peak flux of the lead system. The peak fluxes depend linearly on the incident proton beam energy upto 1 GeV. For higher energies there is only a weak increase of the neutron flux because of the spatial spreading out of the cascades.

In Fig. 2 and 3 the three-dimensional thermal flux distributions for the lead and uranium system at incident proton beam energy of 960 MeV are plotted meshwise. It is obvious that in the uranium case the flux distribution is more concentrated.

Energy MeV	Target	Evaporation Model	Thermal Peak Flux n $cm^{-2}s^{-1}$ per proton	Thermal Peak Flux n $cm^{-2}s^{-1}$ per 1 mA
	Pb	B_0=8,no RAL*	2.4×10^{-2}	1.5×10^{14}
540	Pb	B_0=14, RAL	2.15×10^{-2}	1.34×10^{14}
	U_{dep}	B_0=14, RAL	4.15×10^{-2}	2.59×10^{14}
	Pb	B_0=8,no RAL	4.7×10^{-2}	2.9×10^{14}
960	Pb	B_0=14, RAL	3.55×10^{-2}	2.2×10^{14}
	U_{dep}	B_0=8, RAL	8.9×10^{-2}	5.5×10^{14}
	U_{dep}	B_0=14, RAL	7.8×10^{-2}	4.8×10^{14}
	Pb	B_0=8,no RAL	6.25×10^{-2}	3.9×10^{14}
1470	Pb	B_0=14, RAL	5.1×10^{-2}	3.2×10^{14}
	U_{dep}	B_0=14, RAL	1.1×10^{-1}	6.9×10^{14}

* RAL = High Energy Fission Model /3/ of Rutherford and Appleton Laboratories

Table 1: Calculated thermal neutron peak fluxes for lead and uranium targets for two B_0 values at different incident proton beam energies

Energy	B_0	Peak flux ratio U_{dep}/Pb
540	14	1.93
960	8	1.9
960	14	2.2
1470	14	2.15

Table 2: Energy dependent ratios of thermal neutron peak fluxes for uranium and lead targets

3. NEUTRON SPECTRA COMPARISONS

The calculations are made using the intranuclear-cascade- evaporation model contained in the HETC code in combination with the standard Rutherford and Appleton Laboratory high energy fission model (RAL) with B_0 = 14 /3/. The cases considered are 590-MeV protons on U-238 target nuclei. The measured neutron spectra which are compared with here were kindly provided by S. Cierjacks of KfK, and are unpublished data from experiments performed at SIN. (The experimental method was summarized by Cierjacks, et.al. at ICANS-V /9/.) Cierjacks has indicated /7/ that the normalization of the measured data is to be checked in further experiments at SIN, so the comparisons here should be regarded as preliminary at present. Analyzed data for U targets at three angles (30, 90, and 150 degrees) are compared.

Figures 4-6 show comparisons of the present calculations and the KfK measurements for neutron spectra at 30^{o}, 90^{o}, and 150^{o} from thin uranium targets bombarded by 590-MeV protons.

To show better the low-energy neutron comparisons in the evaporation region, Fig. 7 gives the low-energy (< 10 MeV) neutron part of spectra with a linear scale. The calculated spectra here are averaged over all emission angles.

The basic conclusions from these comparisons are: (a) For uranium, there is rather good agreement in the evaporation region of the spectrum (few MeV and below). The magnitudes of the evaporation peaks agree within 25 %. The evaporation neutron maximum is lower in the calculations (1 MeV calculated vs. 2 MeV measured). In the "region of overlap" of the high-energy part of the evaporation spectrum and where the cascade production begins to dominate (i.e., in the energy range 10 - 25 MeV), the calculated

results are higher, by as much as a factor of 3 at 10 MeV. The high-energy part of the spectrum (> 50 MeV) is underestimated by the calculations, by a factor of 3 for small (e.g., 30^{o}) angles, with much worse agreement at the higher angles.

4. RESIDUAL MASS DISTRIBUTIONS IN THIN URANIUM TARGETS

The calculations made here are for proton beams having kinetic energies of 0.3, 1.0, and 2.9 GeV incident on thin U-238 targets. These were made using the Rutherford and Appleton Laboratory (RAL) high energy fission model and the results computed here are compared with available results for the same cases computed by the Oak Ridge National Laboratory (ORNL) model developed by Alsmiller, et.al. /4/.

A summary of the mass distribution results for the three beam energies as calculated using the RAL model is shown in Figure 8. The points shown are averages over $\Delta A = 5$ intervals, and are plotted at the midpoint of the intervals. Representative error bars (one standard deviation) are indicated. The normalization is per nonelastic proton-uranium collision, which can be converted from yields to production cross sections by multiplying by the computed total nonelastic cross section (Table 3). Note from Fig. 8 that the model predicts a "bump" in production in the mass region between that of the fission products ($A < 180$) and the mass region of the residual spallation product mass in which fission did not occur ($A > 220$); this is discussed in more detail later.

In Figures 9 and 10 results from the RAL model are compared with ORNL model predictions and measured data. The ORNL calculations are also averaged over $\Delta A = 5$ intervals. The normalization of the

measured data of Stevenson, et.al. /10/ at 300 MeV is taken from the ORNL paper /6/, in which the area under the experimental points in the mass region from 60 to 160 was normalized to be the same as the area under the ORNL calculated histogram in this mass region. (The 2.9 GeV experimental values are the absolute production cross sections given by Friedlander, et.al. /11/, converted to yields using the calculated nonelastic cross section.)

From Figures 9 and 10, the model predictions and measured data are all in good agreement in the vicinity of the peaks of the fission fragment mass distributions, although the RAL model seems to predict a somewhat wider fission fragment distribution.

As noted earlier, the RAL model predicts three peaks in the mass distribution: the fission fragment peak near A=110, the spallation peak near A=238, and an intermediate peak near A=200. This intermediate peak apparently results from spallation products which "survive" de-excitation through the mass region of high-fission probability into a lower mass region where further de-excitation by neutron emission is much more likely than fission. For illustration the mass distributions are calculated with and without fission competition for the 1-GeV beam case (Fig. 11). To get the fission probability versus mass number, subroutines of the RAL model are used to compute the fission probability for various arbitrarily selected isotopes covering the mass range from 175 to 250. Thus, while spallation products are produced down to A=160 (for 1-GeV, Fig. 11), and the model allows fission for these low masses, the fission probability determined for these masses is very small for A $<$ 200, accounting for the peak in this region. This intermediate peak in the mass distribution is probably most evident at "medium" beam energies - i.e. at low beam energies (say, 100 MeV) there is not sufficient excitation energy to produce many nuclei in the lower mass region of low-

fission probability, whereas at high beam energies there is sufficient excitation energy that spallation products can be produced with very low masses which overlap with the higher mass fission fragments (as evidenced by the 2.9 GeV results).

Apparently, the ORNL model does not predict an intermediate peak in the mass distribution (Fig. 9), which seems somewhat surprising since the ORNL model neglects fission for nuclei having atomic numbers less than 91.

The results above were computed using a value of 14 for the parameter B_0 in the level density formula, which is the standard value incorporated in the RAL model program. As calculations with different B_0-parameters pointed out, the value of B_0 used has an important effect on neutron production, but has little influence on residual mass distributions.

	Proton Energy		
	0.30 GeV	1.0 GeV	2.9 GeV
σ_{nonel} (barns)	1.75	1.92	1.88
σ_f (barns)	1.38	0.93	0.92
$P_f = \sigma_f/\sigma_{nonel}$	0.79	0.48	0.49

Table 3: Calculated Nonelastic and Fission Cross Sections for Protons on U-238

5. CONCLUSIONS

For the thick target-moderator systems (large H_2O moderator) using lead and uranium as target material a factor of about 2 between uranium (0.2 % wt ^{235}U) and lead in thermal neutron peak fluxes is reachable. The B_0-dependence in lead target systems is larger than in uranium system, therefore in the new KFA version of HETC (HETC/KFA-1) mass dependent level density parameters in the evaporation model were introduced.

From the comparisons of neutron spectra calculations with measurements on this uranium targets the major deficiency of the present model is considered to be the underestimate of the high-energy neutrons. The comparisons here are with preliminary experimental data, and with only a small part of the KfK data which have been taken, so the magnitude of the experimental/theoretical differences may change if further comparisons are made. However, there is enough evidence from these, and other comparisons which have been made, to believe that the difference, at least at large angles, is real, even though the magnitude may be considered still questionable.

The RAL model predicts a somewhat wider fission fragment distribution than the experiment. Between the fission fragment peak and the spallation peak the RAL model predicts an intermediate peak near A=200. This peak results from spallation products which "survive" de-excitation through the mass region of high-fission probability into a lower mass region where further de-excitation by neutron emission is much more likely than fission. The ORNL model does not predict an intermediate peak in the mass distribution which seems somewhat surprising since the ORNL model neglects fission for nuclei having atomic numbers less than 91.

6. REFERENCES

/1/ T.W. Armstrong, P. Cloth, D. Filges, R.D. Neef, "A Comparison of High-Energy Fission Models for the HETC Transport Code, Part II: Thick Targets", Proceedings of the 5th Meeting of the International Collaboration on Advanced Neutron Sources", G.S. Bauer and D. Filges (Eds.), 22-26 June 1981, Jülich, Jül-Conf-45 (October 1981)

/2/ T.W. Armstrong, D. Filges, "A Comparison of High-Energy Fission Models for the HETC Transport Code, Part I: Thin Targets", Proceedings of the 5th Meeting of the International Collaboration on Advanced Neutron Sources", G.S. Bauer and D. Filges (Eds.), 22-26 June 1981, Jülich, Jül-Conf-45 (October 1981)

/3/ F. Atchison, "The Inclusion of Fission in the High-Energy Particle Transport Code, HETC", Bulletin of the American Physical Society 24, 874 (1979)

/4/ F.S. Alsmiller, R.G. Alsmiller Jr., T.A. Gabriel, R.A. Lillie, J. Barish, "A Phenomenological Model for Particle Production from the Collisions of Nucleons and Pions with Fissile Elements at Medium Energies", ORNL/TM-7528 (1981)

/5/ J.S. Fraser, et.al., "Neutron Production in Thick Targets Bombarded by High-Energy Protons", Phys. in Canada 21, 17 (1965)

/6/ R.G. Alsmiller Jr., T.A. Gabriel, J. Barish, F.S. Alsmiller
"Neutron Production by Medium Energy (1.5 GeV) Protons
in Thick Uranium Targets"
ORNL/TM-7527 (1981)

/7/ S. Cierjacks,
KfK unpublished, private communication 1981

/8/ T.W. Armstrong, P. Cloth, D. Filges, R.D. Neef,
"Theoretical Target Physics Studies for the SNQ
Spallation Neutron Source", Jül-Spez-120 (July 1981)

/9/ S. Cierjacks, et.al., "High-Energy Particle Spectra
Spallation Targets", Proceedings of the 5th Meeting
of the International Collaboration on Advanced
Neutron Sources, G.S. Bauer and D. Filges (Eds.)
22-26 June 1981 Jülich, Jül-Conf-45 (October 1981)

/10/ P.C. Stevenson, et.al., "Further Radiochemical
Studies of the High-Energy Fission Products",
Phys. Rev. 111, 886 (1958)

/11/ G. Friedlander, "Fission of Heavy Elements by High-
Energy Protons, in Physics and Chemistry of Fission",
1965, International Atomic Energy Agency, Vienna, 1965

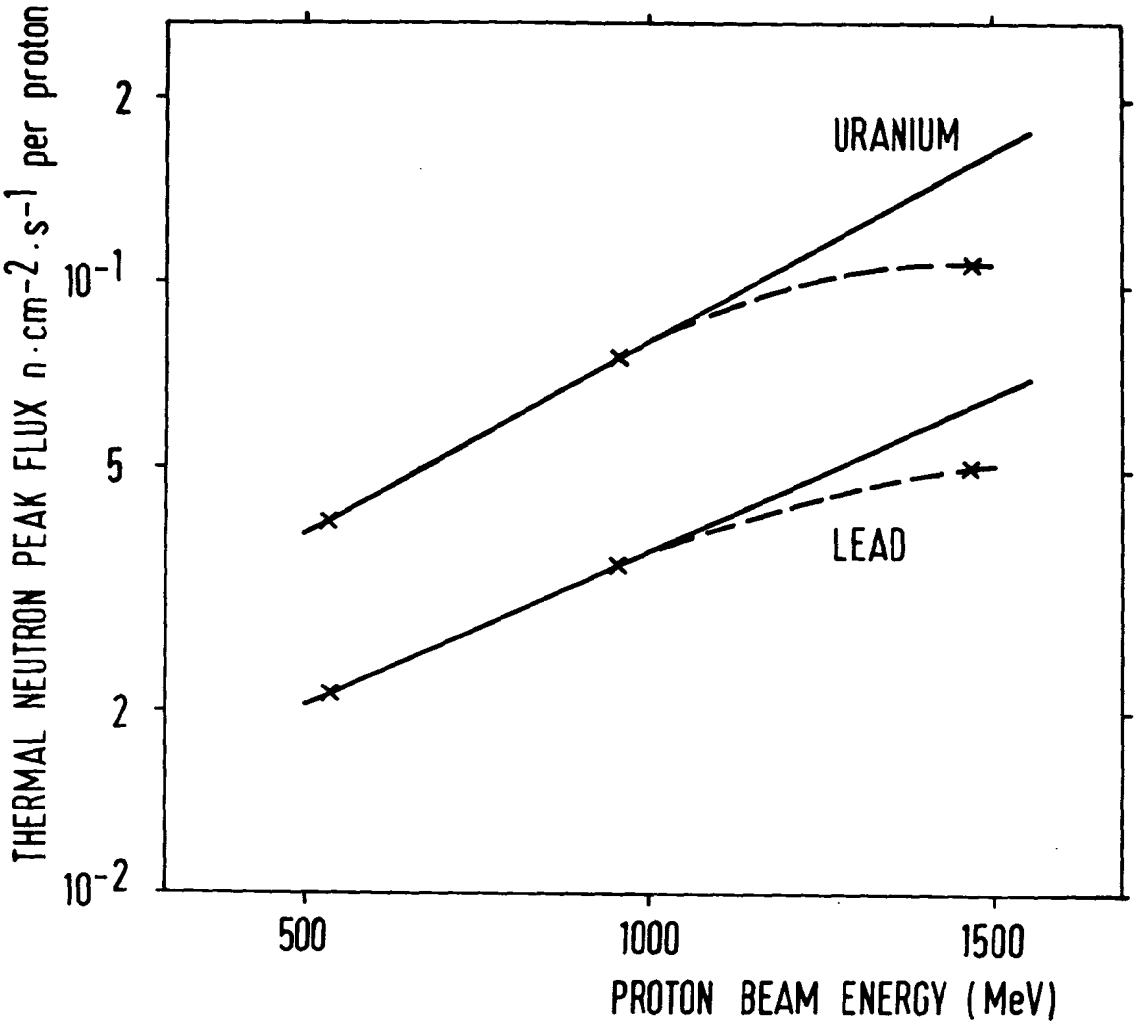

Fig. 1

Thermal neutron peak fluxes per proton as a function of proton beam energy (540, 960, 1470 MeV) for lead and uranium target with B_0 = 14 MeV

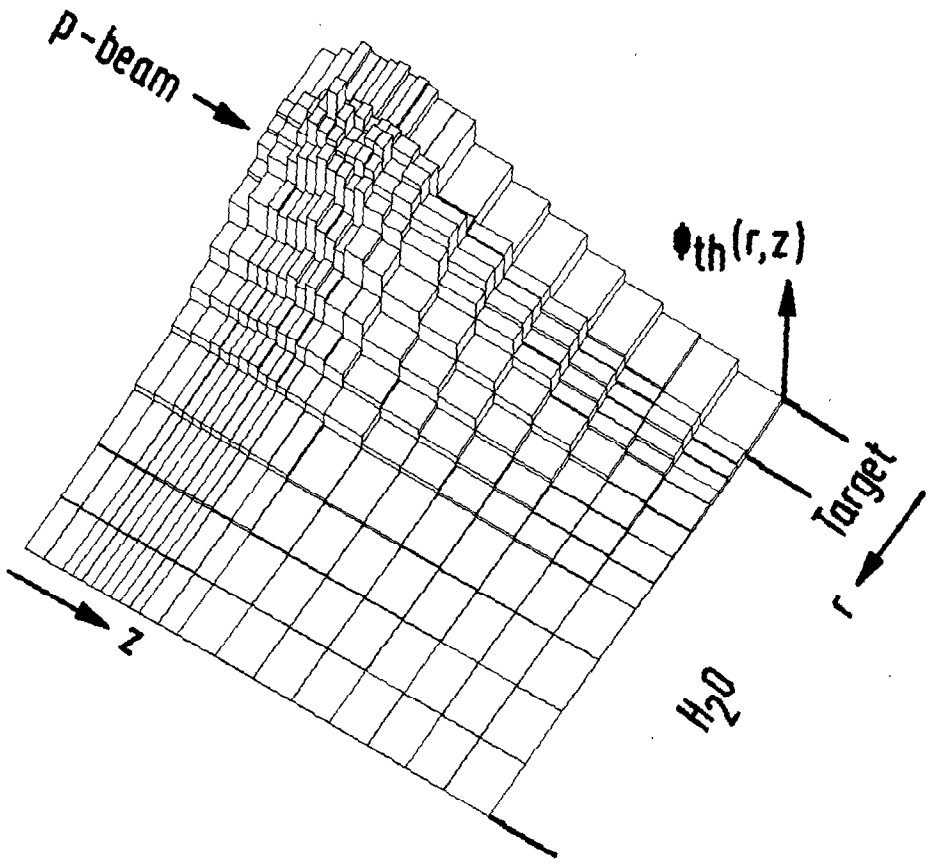

Fig. 2

Thermal neutron flux distribution for the lead system in R-Z plane (incident proton beam energy 960 MeV)

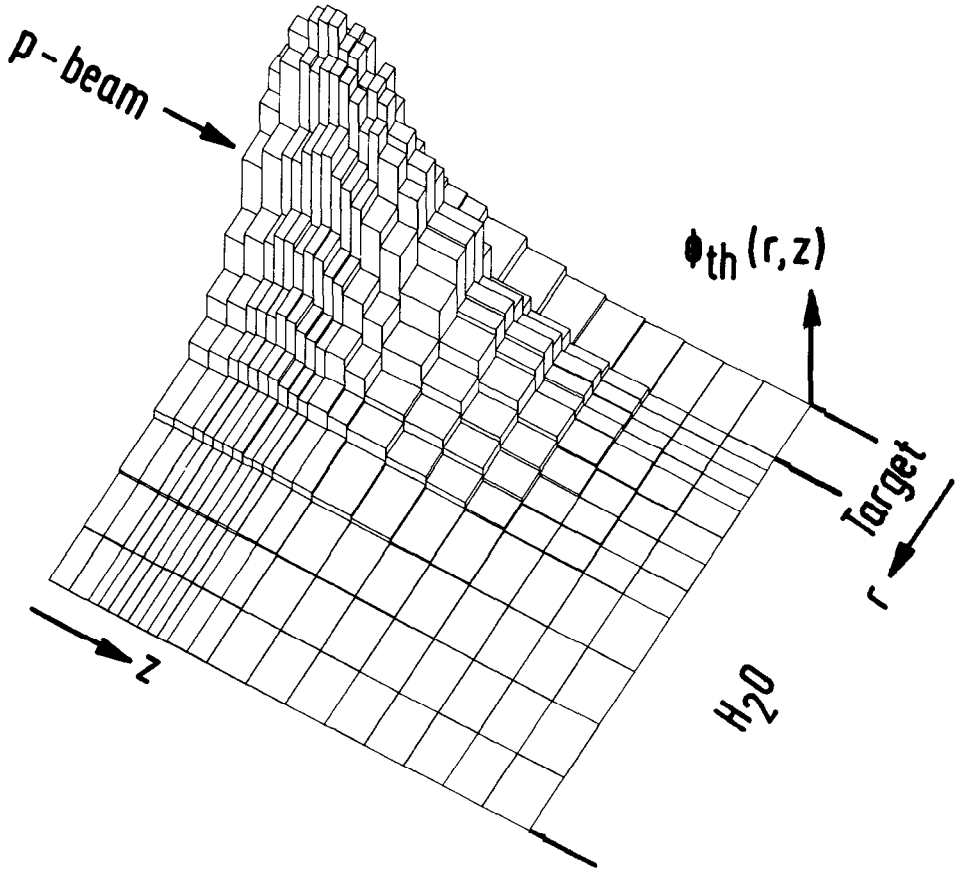

Fig. 3

Thermal neutron flux distriution for the uranium system in R-Z plane (incident proton beam energy 960 MeV)

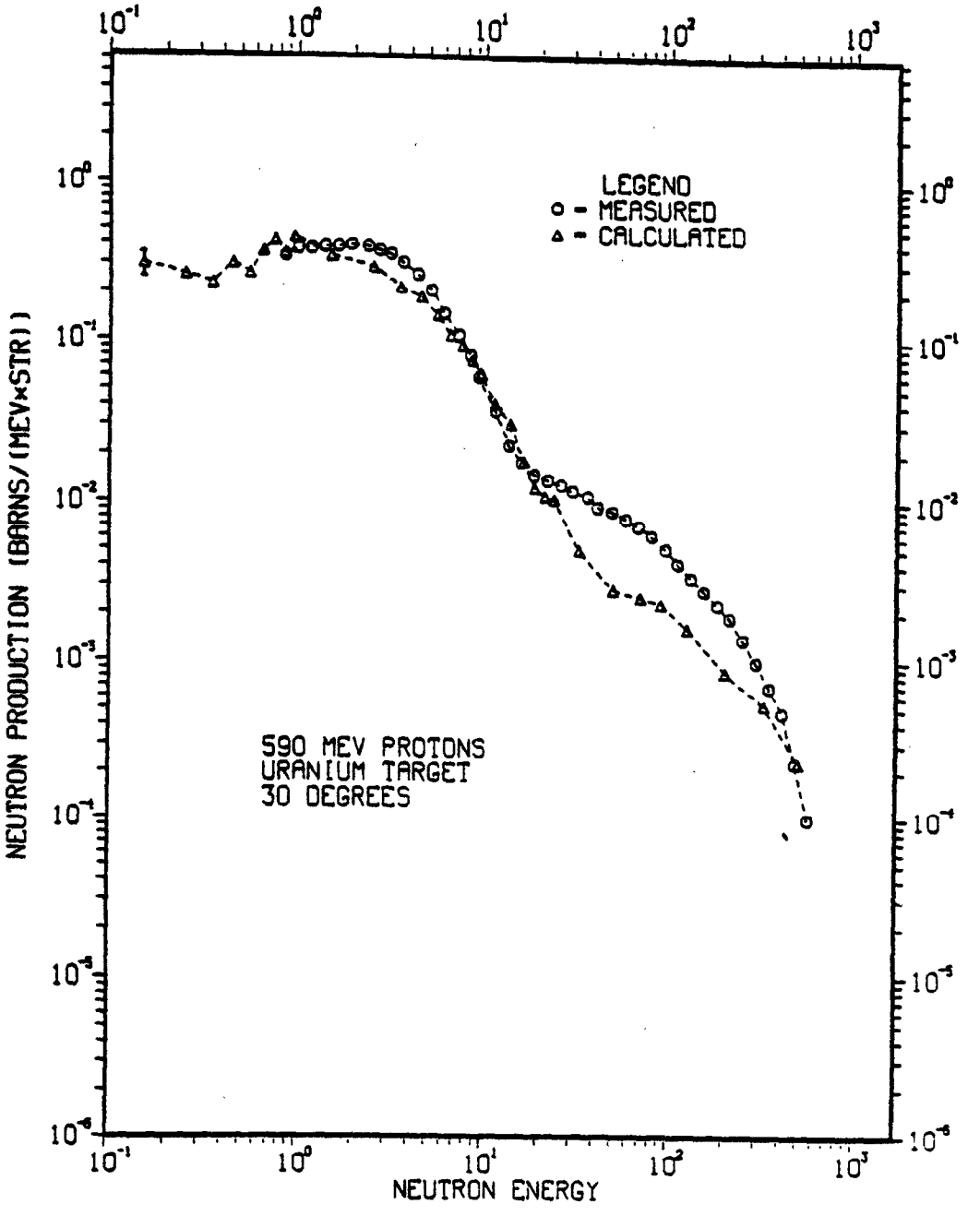

Fig. 4

Comparison of calculated and KfK measured neutron spectra at 30° from uranium target bombarded by 590-MeV protons

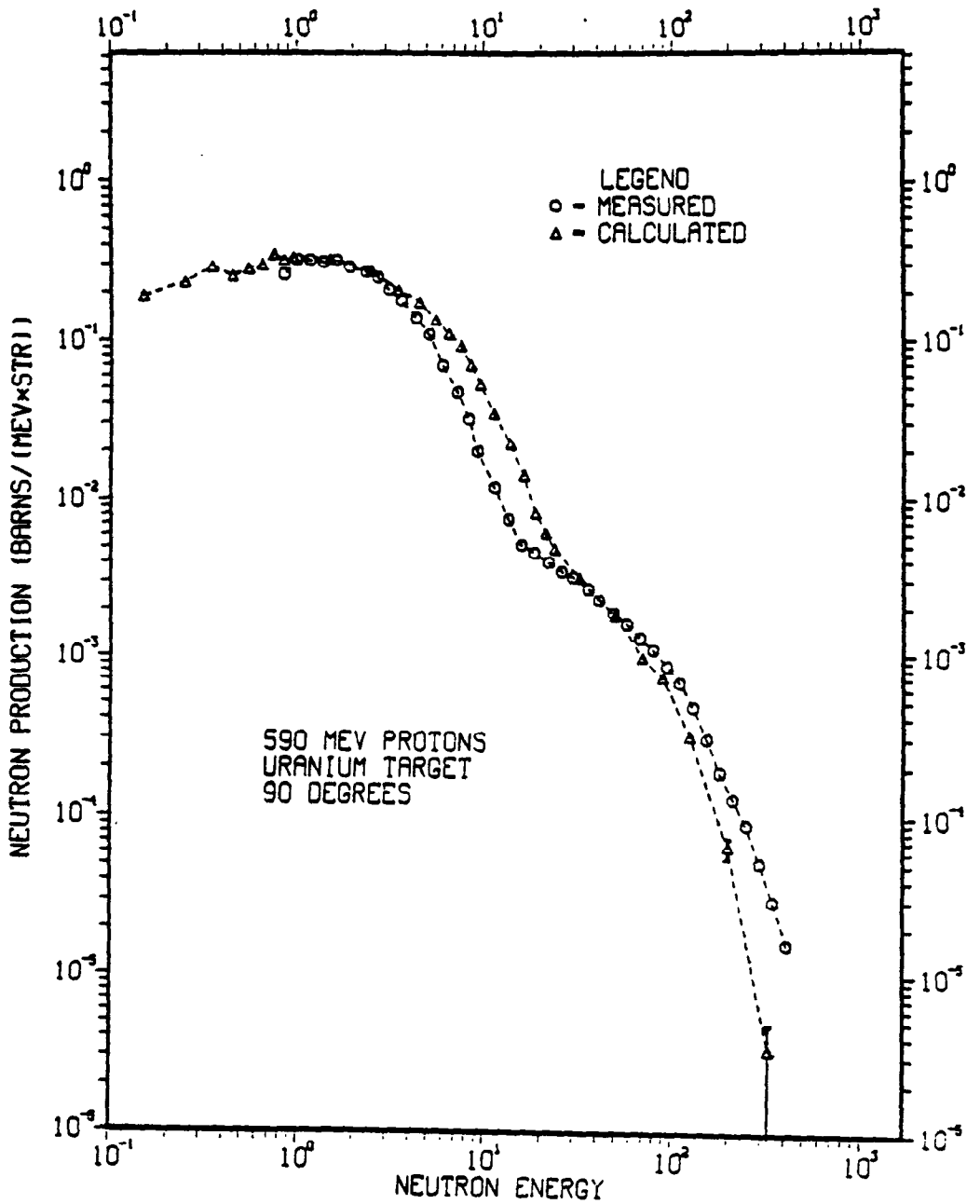

Fig. 5

Comparison of calculated and KfK measured neutron spectra at 90° from uranium target bombarded by 590-MeV protons

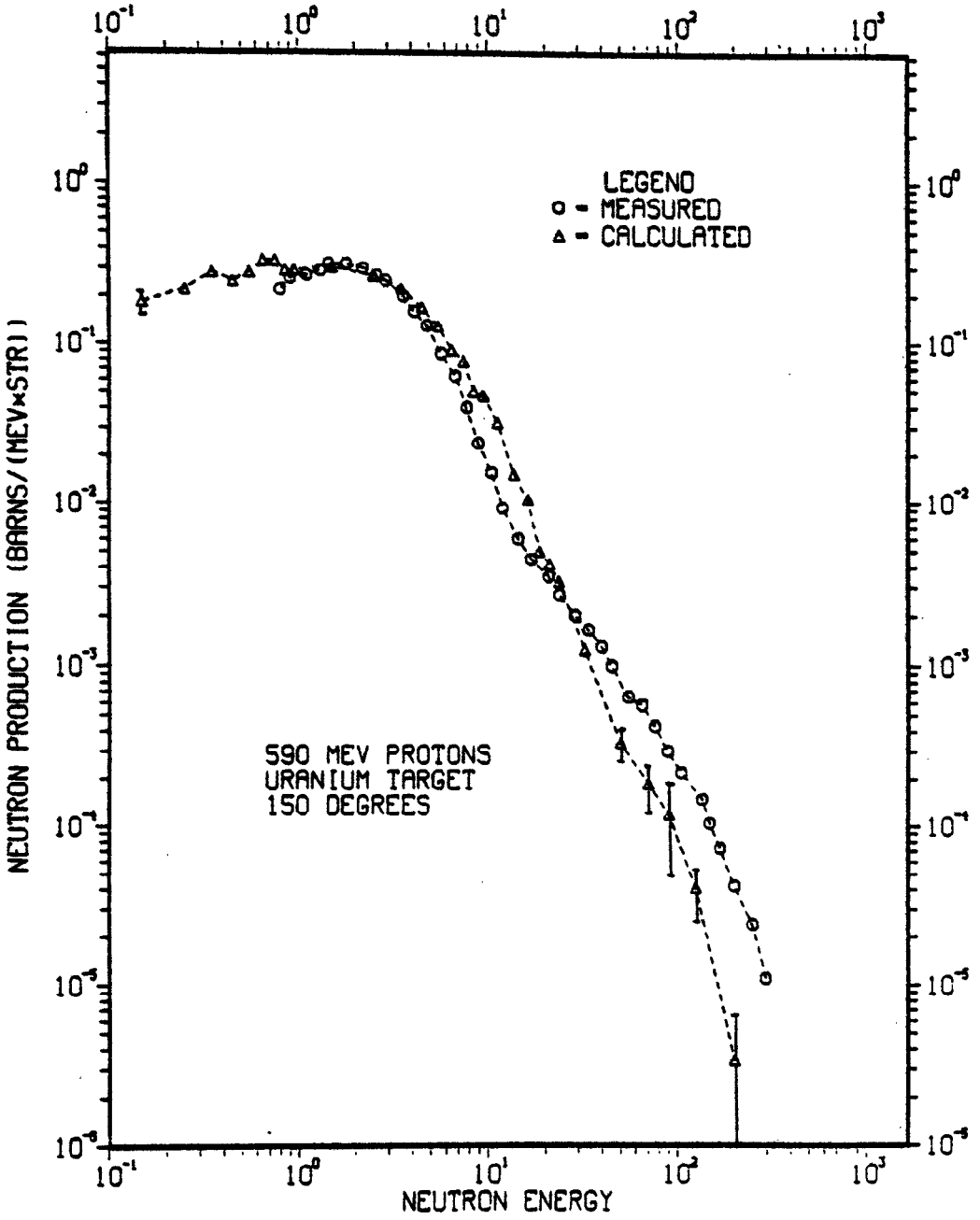

Fig. 6

Comparison of calculated and KfK measured neutron spectra at 150° from uranium target bombarded by 590-MeV protons

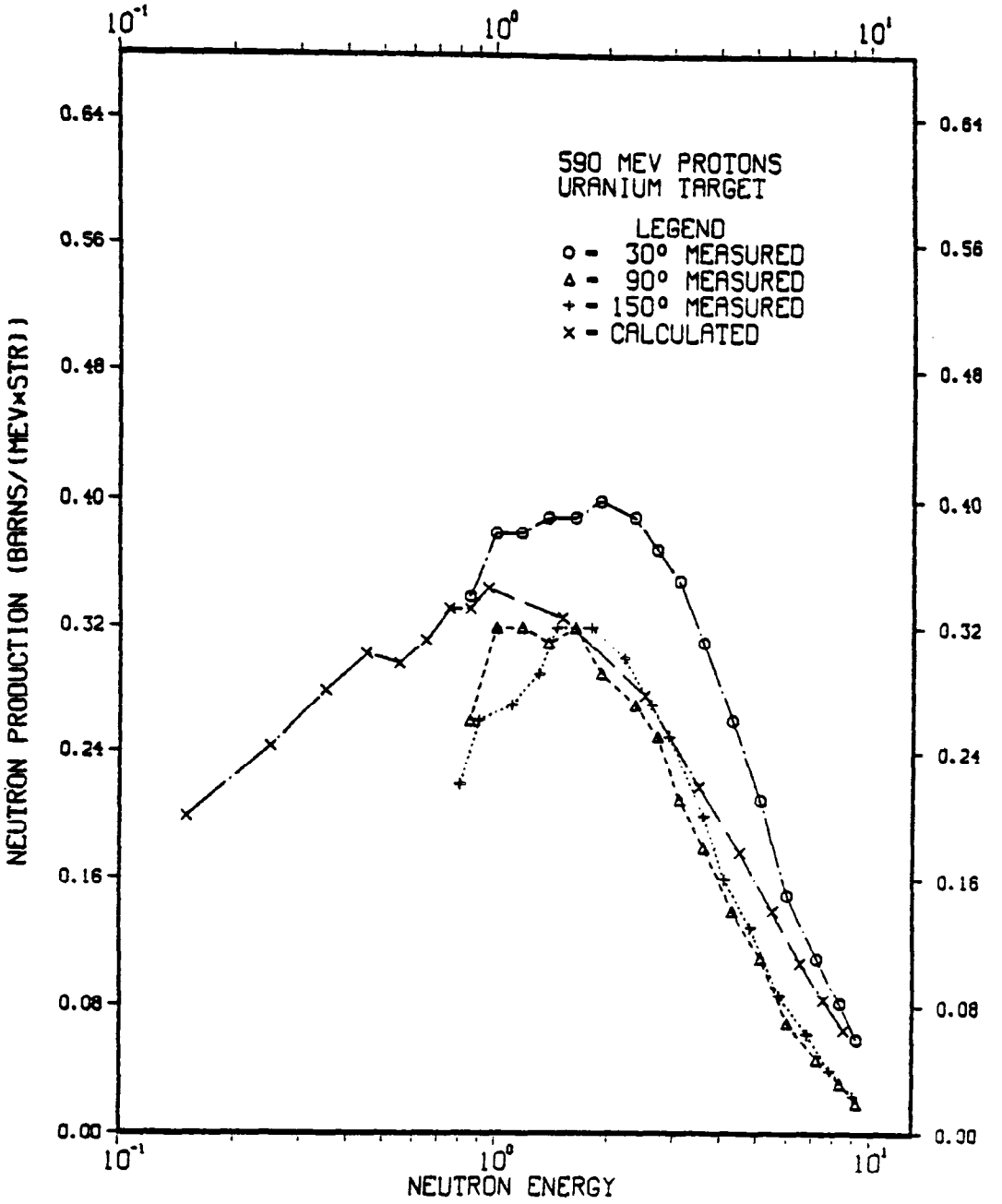

Fig. 7

Comparison of calculated and KfK measured neutron spectra at low energies from a thin uranium target bombarded by 590-MeV protons. The calculated spectrum is averaged over all emission angles

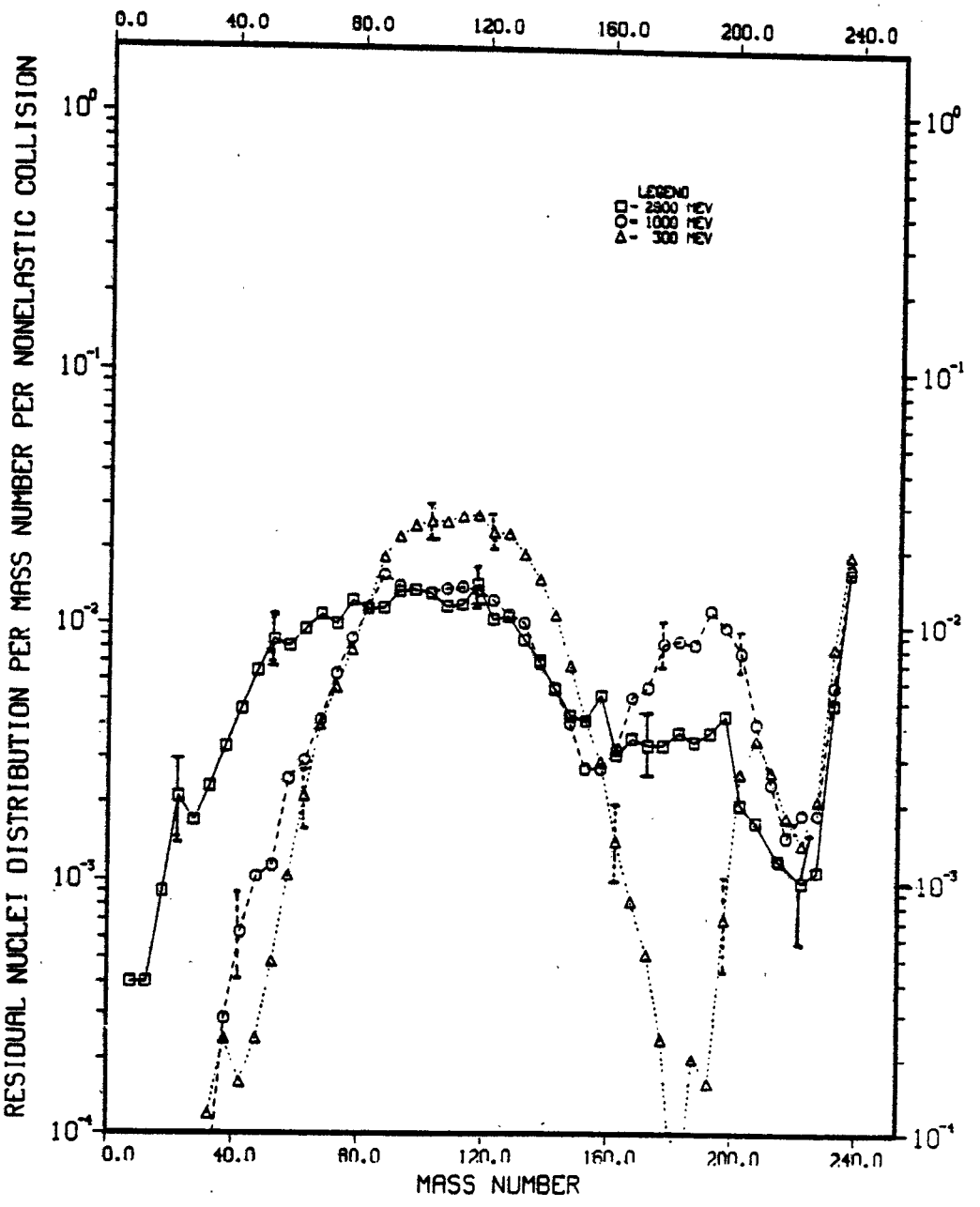

Fig. 8

Mass distributions predicted by RAL high-energy fission model for 300, 1000, and 2900 MeV protons on thin U-238 target

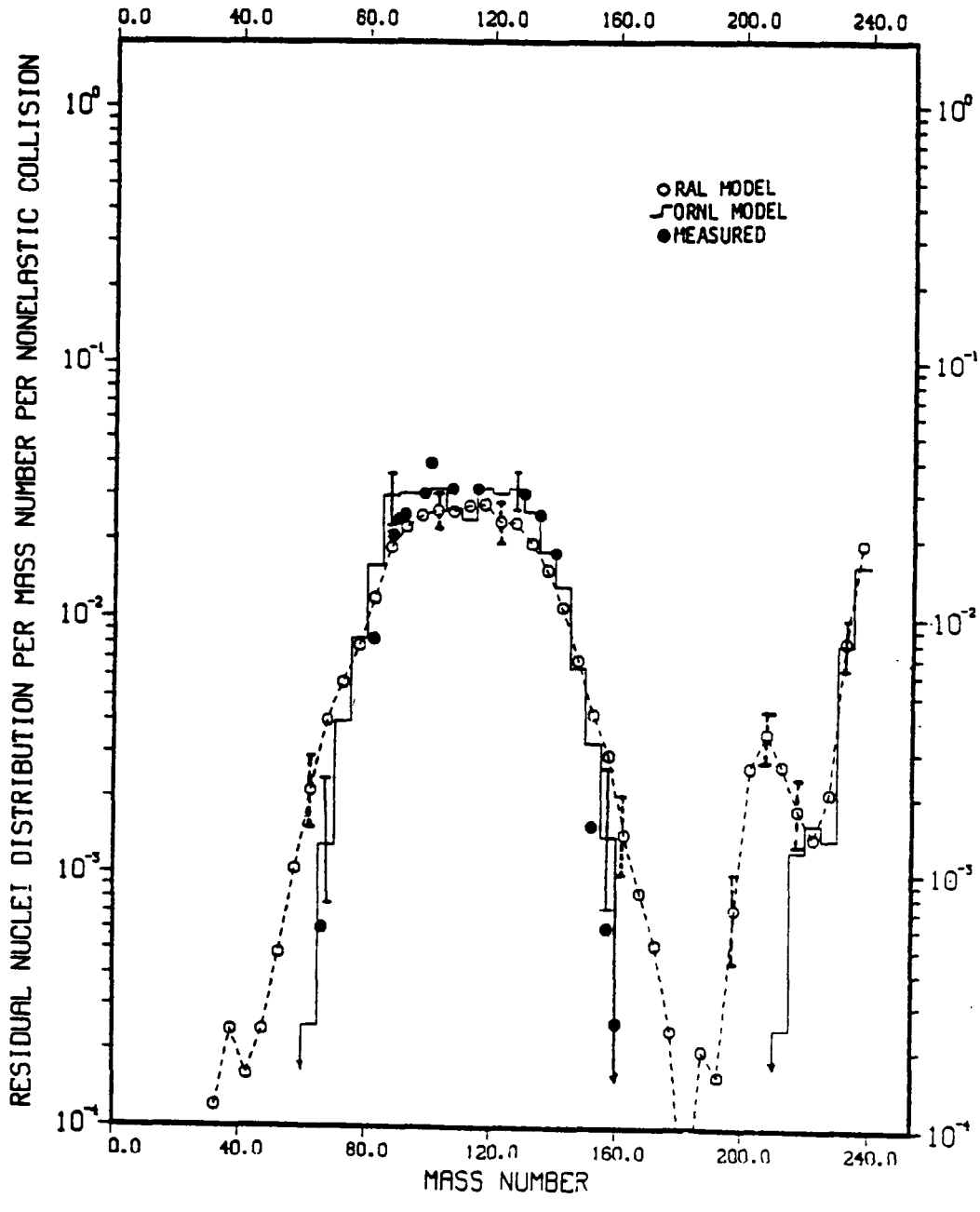

Fig. 9

Comparison of mass distributions computed using RAL model, from ORNL model calculations /6/, and from measurements of Stevenson, et.al. /10/ for 300 MeV protons on thin U-238 target

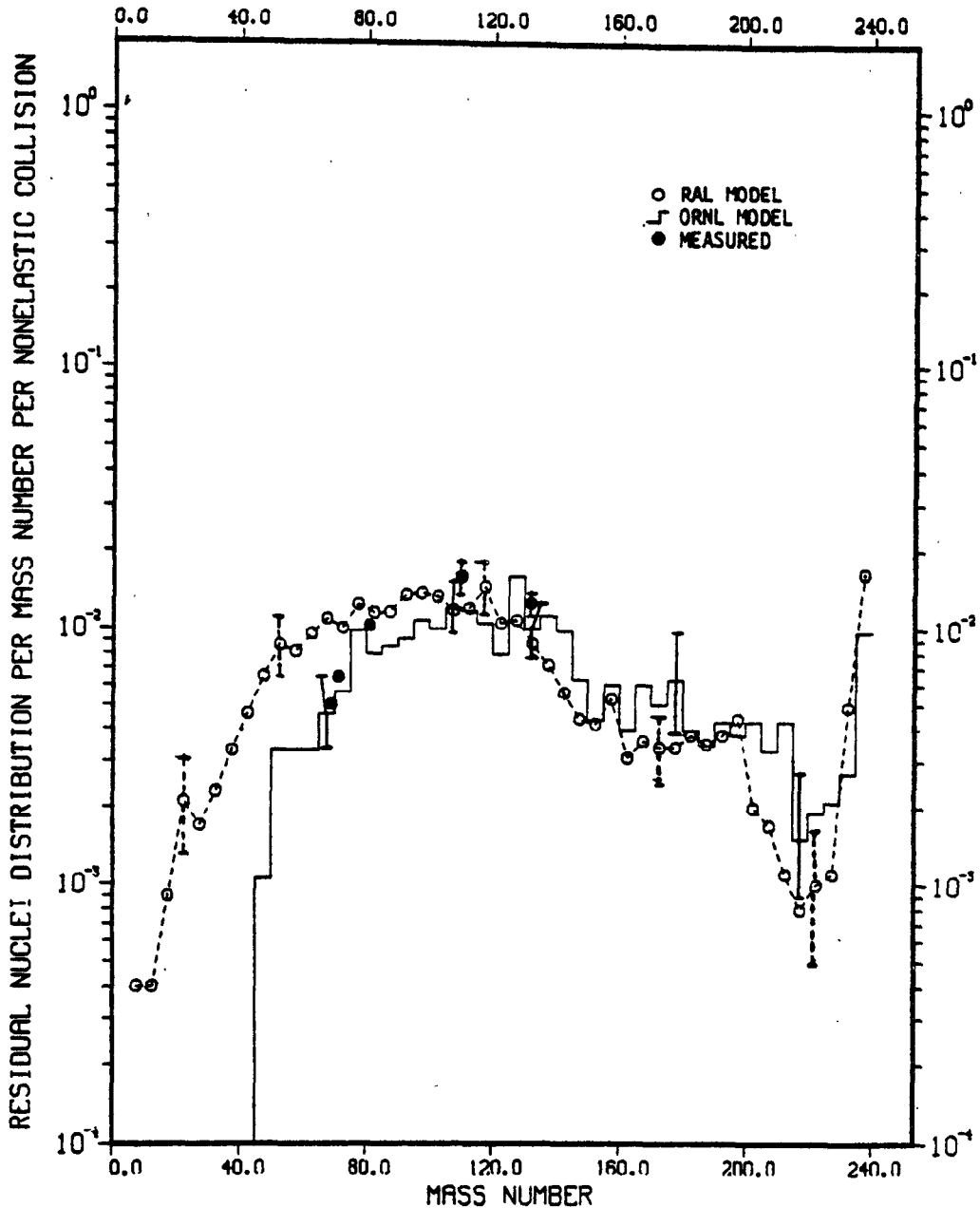

Fig. 10

Comparison of mass distributions computed using RAL model, from ORNL model calculations /6/, and from measurements of Friedlander, et.al. /11/ for 2900 MeV protons on thin U-238 target

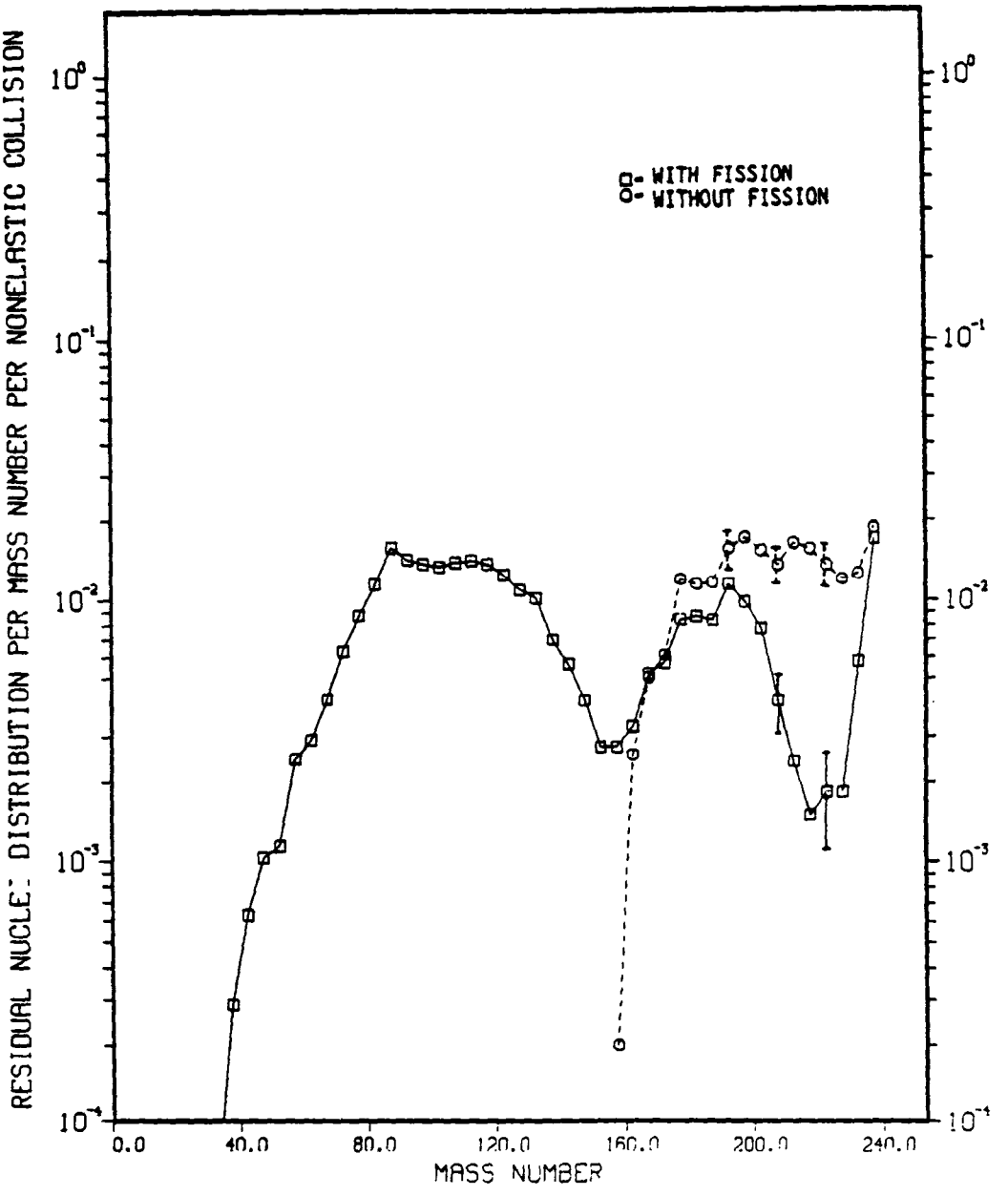

Fig. 11

Comparison of mass distributions with and without high-energy fission taken into account for 1-GeV protons on U-238